Supplementary Information

Interferon Regulatory Factor 8 Modulates Phenotypic Switching of Smooth Muscle Cells through Regulating the Activity of Myocardin

Shu-Min Zhang,[a,b] Lu Gao,[c] Xiao-Fei Zhang,[d] Ran Zhang,[e] Li-Hua Zhu,[a,b] Pi-Xiao Wang,[a,b] Song Tian,[a,b] Da Yang,[a,b] Ke Chen,[d] Ling Huang,[a,b] Xiao-Dong Zhang,[d] Hongliang Li[a,b*]

Department of Cardiology, Renmin Hospital of Wuhan University, Wuhan 430060, China [a]; Cardiovascular Research Institute of Wuhan University, Wuhan 430060, China [b]; Department of Cardiology, Institute of Cardiovascular Disease, Union Hospital, Tongji Medical College, Huazhong University of Science and Technology, Wuhan, PR China [c]; College of life sciences, Wuhan University, Wuhan 430072, China [d]; State Key Laboratory of Medical Molecular Biology, Department of Biochemistry and Molecular Biology, Institute of Basic Medical Sciences, Chinese Academy of Medical Sciences & Peking Union Medical College, Beijing 100005, China[e]

Running title: IRF8 in SMC phenotypic switching

#Address correspondence to Hongliang Li, lihl@whu.edu.cn

S-M. Z., L. G. are co-first authors.

Supplementary Table S1-2

Supplementary Figures S1-4

Supplementary Tables

Table S1 . The primers for making constructs.

Primer name	Primer sequence (5′-3′)
IRF8-5'	CCGGAATTCATGTGTGACCGGAACGGCGG
IRF8-3'	CCGCTCGAGTTAGACGGTGATCTGTTGATT
IRF8-N-3'	CCGCTCGAGTTATGCCACGCCCAGCTTGCATTTT
IRF8-Pro-5'	CCGGAATTCTACCGAATTGTCCCCGAGGAA
IRF8-Pro-3'	CCGCTCGAGTTATGAATGGTGTGTGTCATAGG
IRF8-C-5’	CCGGAATTCTCAGCTTTCTCCCAGATGGTC
MyoD-5'	CCGCTCGAGATGACACTCCTGGGGTCTGAG
MyoD-3'	CCGCTCGAGCTACCACTGCTGCAAGTGAAG
MyoD-N-3'	CCGCTCGAGCTAATCCATCTGCTGACTCCGGGT
MyoD-C-5'	CCGCTCGAGCAGCAGATGGATGAACTCCTG

Sites for restriction enzyme are underlined.

Table S2 . The PCR primers for ChIP assays.

Primer name	Primer sequence (5′-3′)
SM22-1(Forward)	GGAGGTGCTGGAGTTCTATGC
SM22-1(Reverse)	AAGGTAAGGCTTTAGTGGTGTCT
SM22-2(Forward)	CCTTGCAGGTTCCTTTGTCG
SM22-2(Reverse)	CCAAGTTGGAGCAGTCTGTCG
SMA1(Forward)	TTTTGATCTAGGCTACCTTTTGC
SMA1(Reverse)	CAGCTGCTTATGGGGATAAACA
SMA2(Forward)	GAGTTTTGTGCTGAGGTCCCT
SMA2(Reverse)	CCTGGGCTGGGGCTACTTA
smoothelinA1 (Forward)	CCCTGCTAGGTGGGATGAAC
smoothelinA1(Reverse)	CTGGGCAGATAAAGTCTGGAGTC
smoothelinA2(Forward)	TCATACTCCCTATTTAGAACTTCGG
smoothelinA2(Reverse)	CACCTGGTCTGTGCCACCTC

Figure legends

Fig.S1. Arterial injury induces intimal hyperplasia and smooth muscle cell phenotypic switching. (A) Hematoxylin and eosin (HE) stained sections showing the structures of the carotid arteries. Black-framed areas in upper panels are magnified and shown as lower panels. Black arrows indicate internal elastic lamina (IEL) and external elastic lamina (EEL) highlighted in dotted lines. IEL indicates the intimal-medial boundary, while EEL indicate the medial-adventitial boundary; M, media; NI, neointima; and black bars indicate 50 μm. The intimal areas and intima/media ratios were quantified. All of the values are presented as the mean values ± SD, and the statistical significance is indicated: compared with the 7 days post-injury group, **P*< 0.05; compared with the 14 days post-injury group, #*P*< 0.05. (B) Immunofluorescent staining showing the expression of PCNA (red in the top panels), cyclin D1 (red in the middle panels) and α-SMA (green in the bottom panels) in arteries at different time points post-injury. For all panels, DAPI (blue) shows the nuclei. The white bar indicates 20 μm. The proportion of PCNA positive cells and the OD values of cyclin D1 and α-SMA fluorescence were also provided. All of values are presented as the mean values ± SD, and statistical significance is indicated as compared with the sham operation group, **P*< 0.05; compared with the 14 days post-injury group, #*P*< 0.05.

Fig.S2. IRF8 deficiency represses SMC proliferation and migration in response to artery injury. (A) Hematoxylin and eosin (HE) stained sections showing the structures of SM22-Cre and SMC-IRF8-KO carotid arteries from mice that underwent a sham operation or wire injury surgery (at 14 after surgery). Black-framed areas in the upper panels are magnified and shown as lower panels. Black arrows indicate internal elastic lamina (IEL) and external elastic lamina (EEL) highlighted in dotted lines. IEL indicates the intimal-medial boundary, while EEL indicate the medial-adventitial boundary; M, media; NI, neointima; and black bars indicate 50 μm. Intimal areas and intima/media ratios were quantified (N=6). (B) Representative immunofluorescent

staining of the VSMCs using anti-SMA antibody (green color). Blue shows nuclei stained with DAPI. (C) Immunofluorescent staining showing PCNA and cyclin D1 (red) expression and localization in WT and IRF8$^{-/-}$ carotid arteries at 14 days and 28 days post-injury. DAPI (blue) indicates nuclei, and the white bar indicates 20 μm. The proportion of PCNA positive cells and the OD values of cyclin D1 were calculated (N=3 to 6 per group at each time point). (D) Levels of PCNA, cyclin D1 and MMP9 protein in WT and IRF8-/- arteries were determined by Western blotting. Arteries harvested from the sham-operation group and the 28 days post-injury group were used. The expression levels were normalized to GAPDH and quantified. Blots are representative of three independent experiments. For (A) to (D), all values are presented as the mean values ± SD, and statistical significance is indicated as compared with the WT group, *P< 0.05. (E) Migration assay of cultured SMCs isolated from WT and IRF8 KO mice. Isolated SMCs were serum-starved for 24 hours, then cultured in a cell migration filter insert, containing media with or without PDGF-BB (20 ng/mL) as a chemoattractant in the lower chamber. Cells migrating across the filters at 6 hours were stained with 0.1% crystal violet/20% methanol (upper panel). Magnification is ×200. Lower panel: cellular migration was determined by counting the cells that migrated through the pores (n=6). Migration experiments were carried out in triplicate and repeated three times. The results are expressed as the mean values ± SD. *P< 0.05 versus PDGF-BB treated WT group.

Fig.S3. SMC-specific IRF8 overexpression promotes SMCs proliferation in response to artery injury. (A) Immunofluorescent staining shows the PCNA and cyclin D1 (red) expression and localization in NTG and SMC-specific IRF8 TG carotid arteries at 14 days and 28 days post-injury. DAPI (blue) marks the nuclei, and the white bar indicates 20 μm. The proportion of PCNA-positive cells and the OD values of cyclin D1 were calculated. (N=3 to 6 per group at each time point). (B) The levels of PCNA, cyclin D1 and MMP9 protein in NTG and TG arteries were determined by Western blotting. Arteries harvested from the sham-operation group and the 28 days post-injury group were used. The expression levels were normalized to GAPDH and quantified.

Blots are representative of three independent experiments. All values are presented as the mean value ± SD, and statistical significance is indicated as compared with the NTG group, *P<0.05.

Fig.S4. IRF8 inhibits myocardin transactivation. (A) Changes in the binding ability of SRF to the CArG promoter following pcDNA3.1-HA-IRF8 and pcDNA3.1 treatment in MOVAS were analyzed using the ChIP qPCR technique. Error bars indicate the mean value ± SD; *P<0.05; Data are derived from three independent experiments. (B) 3×CArG-luciferase (left panel) and SM22α-luciferase (right panel) constructs were introduced into RASMCs cells. EGFP-Myc-IRF8-C construct, whose product cannot interact with myocardin, was used as an IRF8 mutant to determine the requirement of the IRF8-myocardin interaction for inhibiting CArG-dependent gene expression. After infection with Admyocardin, AdIRF8, AdIRF8 (Admutant) or AdGFP, the luciferase activity was analyzed. The data represent the mean values ± SD, compared with myocardin+/IRF8-/mutant- group, *P< 0.05, compared with myocardin+/IRF8+/mutant- group, #P<0.05. (C) p300 and IRF8 plasmids in a gradient of doses were transfected into 3×CArG-luciferase (left panel) and SM22α promoter-luciferase (right panel) containing A7r5 cells, and then the luciferase activity was analyzed. (D) Left panel: CArG-luciferase was introduced into primary RASMCs to evaluate CArG-dependent expression. Luciferase activity was analyzed after Admyocardin, Adp300, AdIRF8 or AdGFP infection. Right panel: The antagonism between p300 and IRF8 was also detected using SM22α-luciferase containing RASMCs. The data represent the mean values ±SD, compared with myocardin+/p300+/IRF8- group, *P< 0.05.

Fig .S1

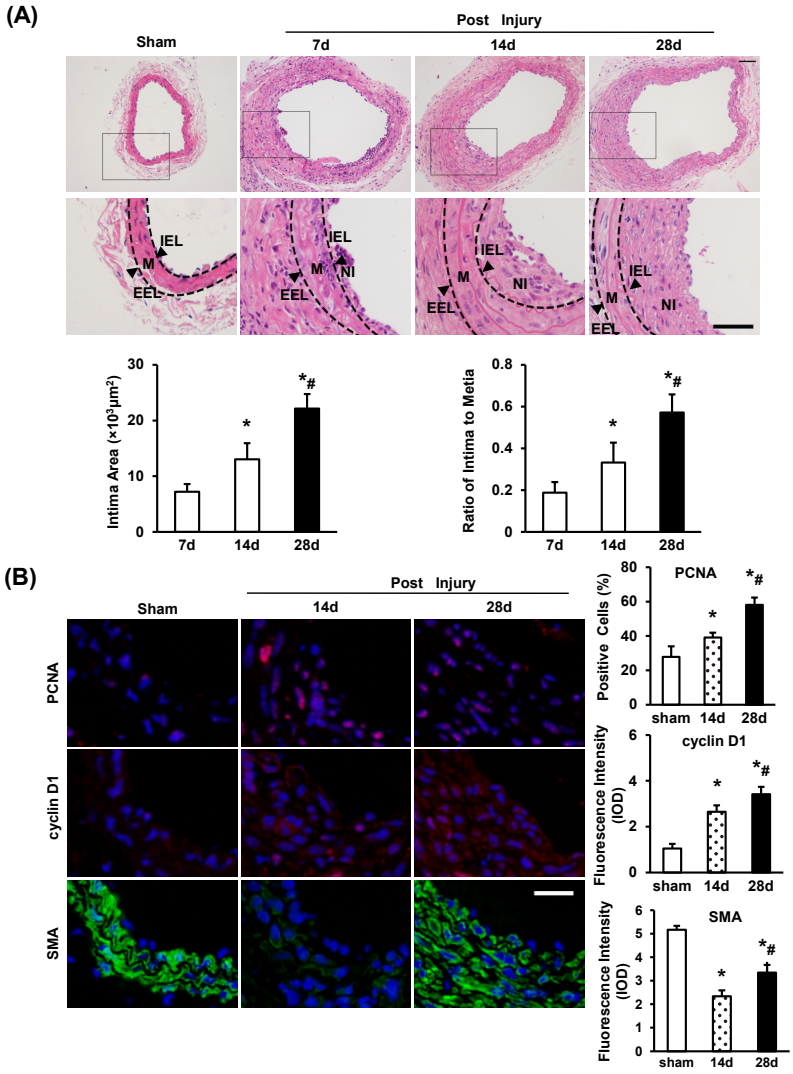
(A)
Sham
Post Injury
7d
14d
28d
IEL
M
EEL
NI
Intima Area (×10³μm²)
Ratio of Intima to Metia
(B)
Sham
Post Injury
14d
28d
PCNA
cyclin D1
SMA
Positive Cells (%)
Fluorescence Intensity (IOD)
sham
14d
28d

Fig.S2

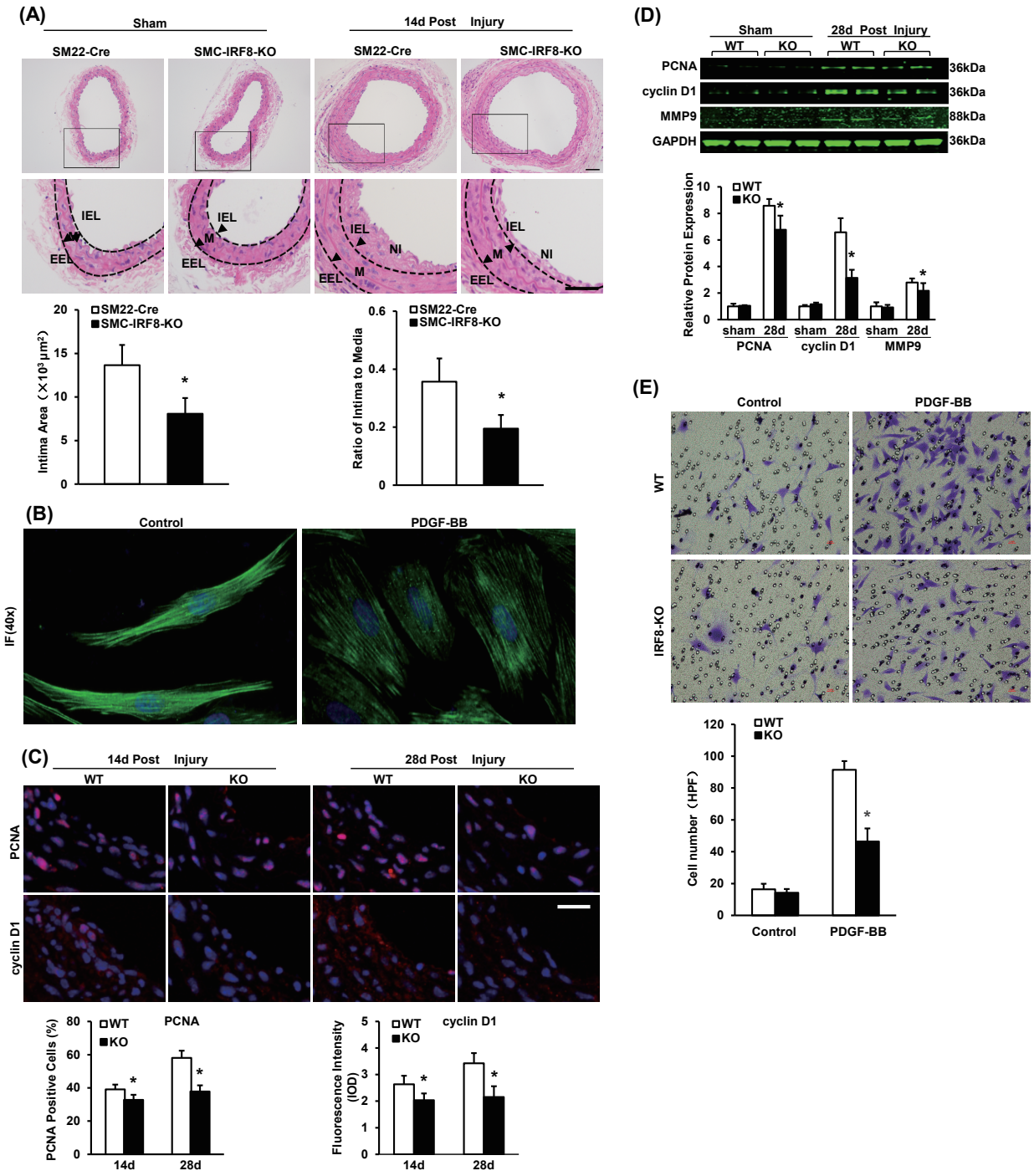
(A)
Sham
14d Post Injury
SM22-Cre
SMC-IRF8-KO
SM22-Cre
SMC-IRF8-KO
IEL
M
EEL
NI
Intima Area (×10³ μm²)
Ratio of Intima to Media
SM22-Cre
SMC-IRF8-KO
(B)
Control
PDGF-BB
IF(40x)
(C)
14d Post Injury
28d Post Injury
WT
KO
PCNA
cyclin D1
PCNA Positive Cells (%)
Fluorescence Intensity (IOD)
14d
28d
(D)
Sham
28d Post Injury
WT
KO
PCNA
cyclin D1
MMP9
GAPDH
36kDa
88kDa
Relative Protein Expression
sham 28d
PCNA
cyclin D1
MMP9
(E)
Control
PDGF-BB
WT
IRF8-KO
Cell number (HPF)

Fig.S3

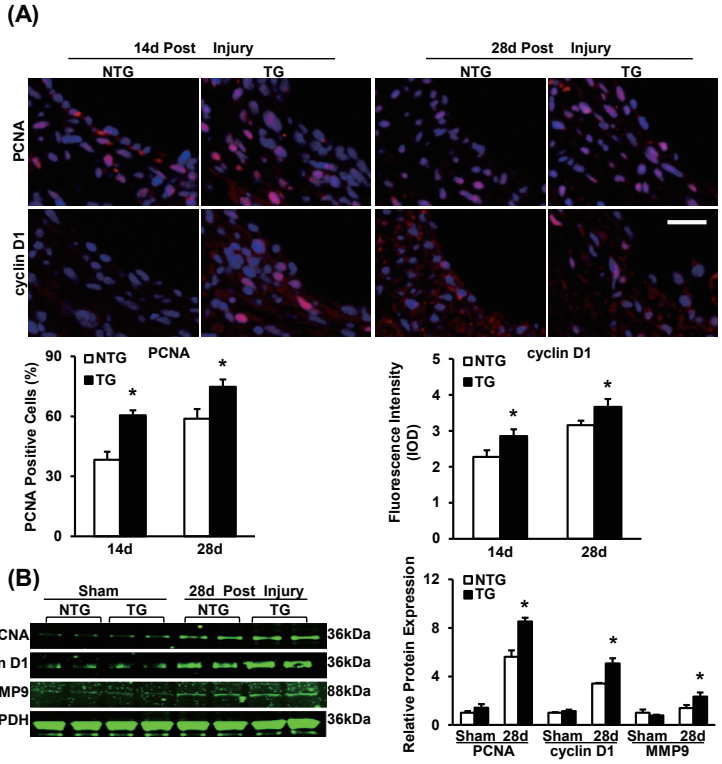
(A)
14d Post Injury
28d Post Injury
NTG
TG
PCNA
cyclin D1
PCNA
NTG
TG
PCNA Positive Cells (%)
90
60
30
0
14d
28d
cyclin D1
Fluorescence Intensity (IOD)
5
4
3
2
1
0
(B)
Sham
28d Post Injury
PCNA
cyclin D1
MMP9
GAPDH
36kDa
88kDa
Relative Protein Expression
12
8
4
Sham 28d
PCNA
cyclin D1
MMP9

Fig.S4

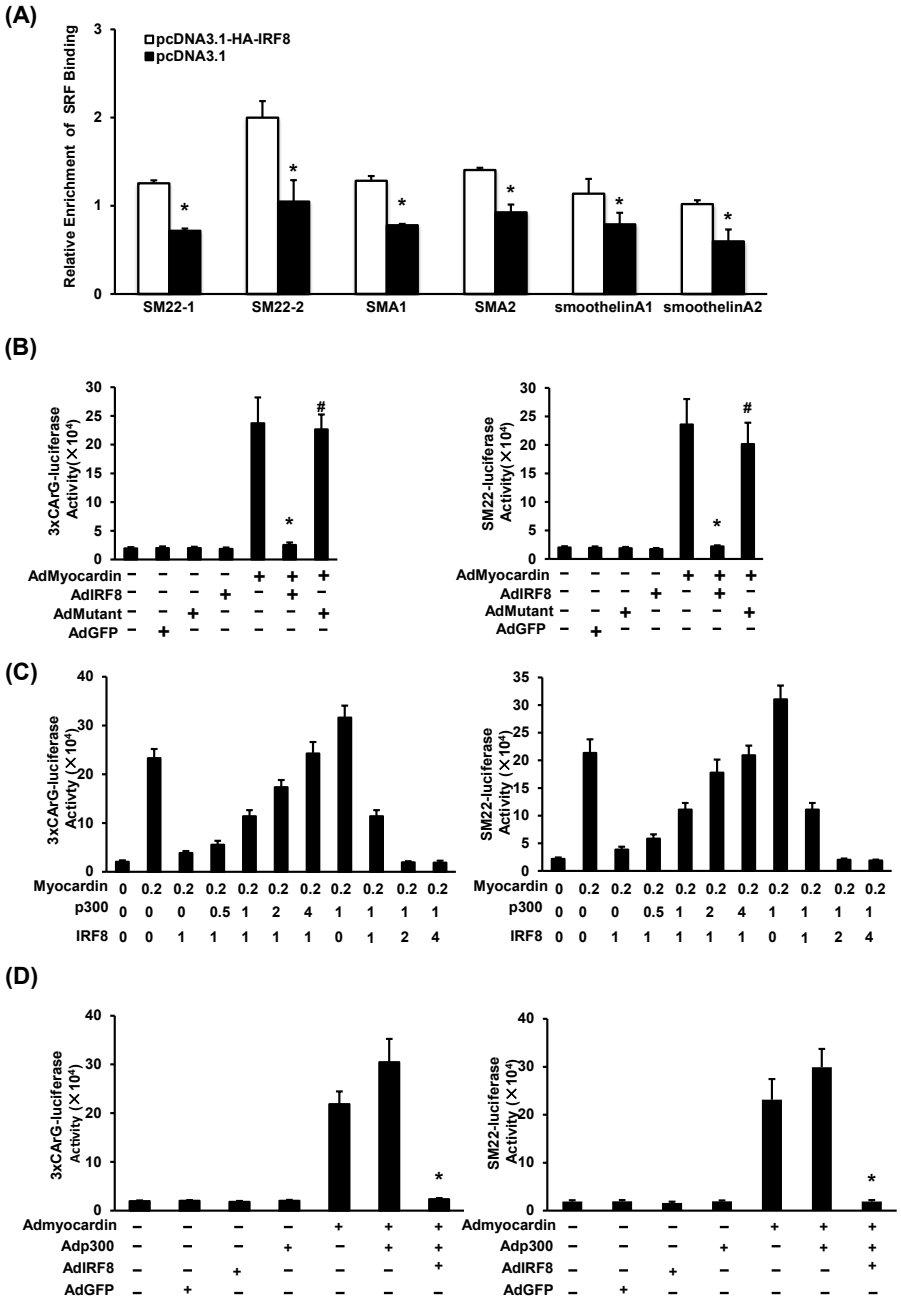
(A)
pcDNA3.1-HA-IRF8
pcDNA3.1
Relative Enrichment of SRF Binding
SM22-1
SM22-2
SMA1
SMA2
smoothelinA1
smoothelinA2
(B)
3xCArG-luciferase Activity(×10⁴)
SM22-luciferase Activity(×10⁴)
AdMyocardin
AdIRF8
AdMutant
AdGFP
(C)
3xCArG-luciferase Activity (×10⁴)
SM22-luciferase Activity (×10⁴)
Myocardin
p300
IRF8
(D)
3xCArG-luciferase Activity (×10⁴)
SM22-luciferase Activity (×10⁴)
Admyocardin
Adp300
AdIRF8
AdGFP